Civil Engineering and Architecture 13(6): 4473-4485, 2025 http://www.hrpub.org
DOI: 10.13189/cea.2025.130626

Static Wind Analysis vs. Wind Tunnel Insights: Understanding the Aerodynamic Behavior of a Tensed Parabolic Structure

Joseph Lenin Adama Arroyo[1], Carlos Javier Huaman Albino[1,*], Nelfa Estrella Ayuque Almidon[2], Juan Gabriel Benito Zuñiga[3]

[1]Faculty of Engineering, Academic School of Civil Engineering, Universidad Continental, Peru
[2]Faculty of Engineering, Universidad Nacional del Centro del Perú, Peru
[3]Faculty of Engineering, Universitat Politècnica de València, Spain

Received September 22, 2024; Revised December 3, 2024; Accepted November 20, 2025

Cite This Paper in the Following Citation Styles

(a): *[1] Joseph Lenin Adama Arroyo, Carlos Javier Huaman Albino, Nelfa Estrella Ayuque Almidon, Juan Gabriel Benito Zuñiga , "Static Wind Analysis vs. Wind Tunnel Insights: Understanding the Aerodynamic Behavior of a Tensed Parabolic Structure," Civil Engineering and Architecture, Vol. 13, No. 6, pp. 4473 - 4485, 2025. DOI: 10.13189/cea.2025.130626.*

(b): *Joseph Lenin Adama Arroyo, Carlos Javier Huamán Albino, Nelfa Estrella Ayuque Almidon, Juan Gabriel Benito Zuñiga (2025). Static Wind Analysis vs. Wind Tunnel Insights: Understanding the Aerodynamic Behavior of a Tensed Parabolic Structure. Civil Engineering and Architecture, 13(6), 4473 - 4485. DOI: 10.13189/cea.2025.130626.*

Abstract Strong winds can damage tensile structures, affecting their functionality and generating economic losses. In Peru, the knowledge of tensile structures for both static and dynamic design against wind actions is limited since the Peruvian standard E.020 (loads) only provides criteria for static wind design but not for dynamic behavior. Loads provide only static wind design criteria but not the dynamic behavior. For that reason, this research is focused on wind dynamics through wind tunnel as an essential complement to the static analysis and its respective comparison. For this purpose, the tensile steel structure was proposed with models of 2, 4, 6, and 8 frames, and an analysis with fundamental parameters, which are the topography factor, aerodynamic form factor, and dynamic response factor, was performed in the software RFEM 5 and RDWIN. Subsequently, the wind speed and pressure established in the E.020 standard were used for recalculation, and then the loads were assigned to generate the finite element mesh, culminating in the wind tunnel simulation. As a result, the 6- and 8-frame models showed better performance when analyzed statically and by wind tunnel, showing lower variations in displacement, shear resistance and factor of safety, while the 2-frame models were found to be more sensitive to wind pressure and displacement. Finally, it is concluded that the consideration of the number of frames influences the behavior of tensile systems by static analysis and the dynamic effect used in wind tunnel analysis.

Keywords Tensile Structures, Static Approach, Wind Tunnel

1. Introduction

Tensile structural systems have established themselves as efficient and innovative architectural solutions, especially in regions with complex geographical conditions, such as the Andes Mountains [1]. These structures show remarkable adaptability and flexibility, but their performance under wind loads is a significant challenge due to the extreme climatic conditions of the region [2]. Comparative evaluation of static wind analysis and wind tunnel simulations is essential to optimize their design and ensure their structural safety [3]. Currently, there are several research studies aimed at understanding tensile structures, which are based on both architectural and structural design. This knowledge is of great relevance for the execution of civil projects, especially with regard to the

behavior against loads induced by wind-structure interaction, as well as the fulfillment of functional requirements and the constraints imposed by the site [4]. On the other hand, there are technological methods that are applied directly to the structures, such as those reported by Marchisotti et al. [5]. To obtain accurate measurements of deformations and displacements during wind tunnel tests, they applied sensors that allow capturing the displacement of the whole structure without the need for markers or opticalinterference. Although these techniques offer low-cost solutions, the lack of calibrations for the study decreases the confidence in their practical application. In this context, computational simulation of wind flow over tensile structures, as presented by Blanco [6], uses tools such as computational fluid dynamics (CFD) and different pressure coefficients [7] to provide more reliable quantitative results. Similarly, the application of simulators such as ETABS software widely used in the academic field allows a fast 3D modeling [10], applied to various tensile structures, such as bridges, tall buildings, for static and dynamic analysis since it is of interest to several engineers [8], to analyze the behavior of high-rise structures against wind. Others have also analyzed [9], at a theoretical level, the tensile structures. These studies use advanced methods such as conjugate gradient and Newton-Raphson to model the nonlinear behavior of the structures. Regarding the problem, the extreme climatic conditions, and the high variability of winds in the Andes Mountains require a rigorous and detailed approach to evaluate the behavior of tensile structures. On the other hand, the Peruvian Technical Standard NTP E.020 [11] limits the design criteria for the static and dynamic analysis of wind in tensile structures, as well as the wind map and its out-of-phase velocity values (see Figure 1).

The scarcity of specific studies in this Peruvian region underlines the importance and urgency of this research. This work aimed to compare two main approaches: static analysis and wind tunnel simulations, with the objective of obtaining a comprehensive understanding of the structural response under loading conditions. Therefore, displacements, tension forces, Load and Resistance Factor Design (LRFD) and Allowable Stress design (ASD) safety factors, wind speed, wind pressure were determined. This integrated approach will contribute to the development of safer and more efficient solutions in the field of civil engineering by optimizing structural design in complex environments such as the Andes Mountains.

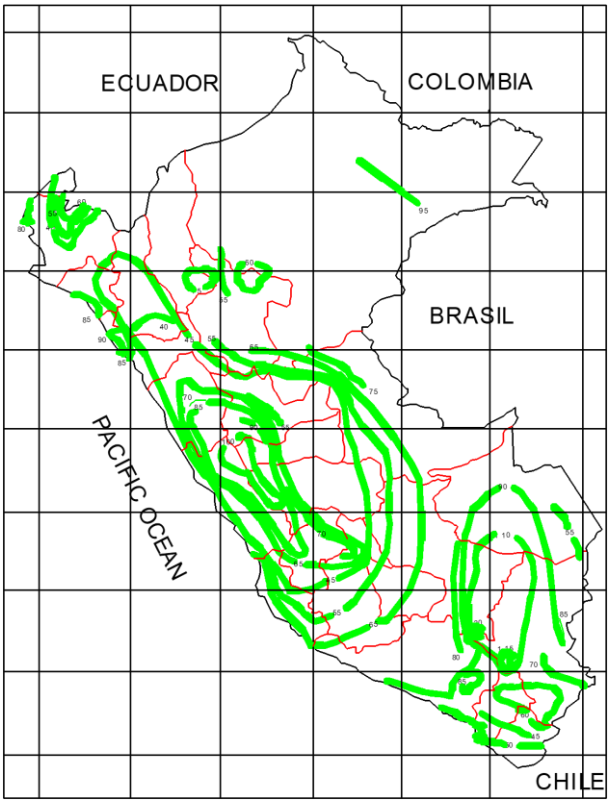

Figure 1. Wind map of Peru

2. Materials and Methods

In this research article, different materials were used such as 6x7 Wc galvanized cable, A500 tubular profiles, and a textile membrane. These are elements that work better in tension and without buckling, since their mechanical properties have a geometric nonlinear behavior according to the kinematic viscosity of 0.000015 m^2/s. The methods used were the static wind analysis of the Peruvian Technical Standard E.020, finite element meshing, computational fluid dynamic (CFD) simulation, Load and Resistance Factor Design (LRFD) and Allowable Stress design (ASD) for metallic coverings.

2.1. Static Wind Analysis

First, the static wind analysis with the design velocity (Vh) at height h and the wind pressure (Ph) at a height h was determined using Equations 1 and 2 [11].

$$V_h = \mathrm{V}(\frac{h}{10})^{022} \quad (1)$$

Where: "Vh" is the design speed as a function of height expressed in km/h, 'V" is the design speed up to 10 m height expressed in km/h and "h" is the height above ground expressed in m.

The wind pressure was continuously determined.

$$P_h = 0.005 \ \ \mathrm{C} \ \ {V_h}^2 \quad (2)$$

Where: "Ph" is the wind pressure or suction as a function of height expressed in kg/m^2, "C" is the dimensionless shape factor and "Vh" is the design speed as a function of height expressed in km/h.

2.2. Mechanical Properties of Materials

The dynamic behavior was analyzed based on static analysis data after defining each material and load. For the Tubular Cross Section (TTS) steels, there are different grades A, B and C, which have a high resistance due to their different shape and thickness. Due to its applicability as structural steel and common use facilitating weldability and formability [11], the type of steel used in the research is A500. In addition, both steel sections have similar strength properties except for the yield strength, which for the tubular steel has a value of 22.75 KN/cm^2 [12]. The following Table 1 shows the mechanical properties of the rectangular A500 steel.

Table 1. Mechanical properties of tubular and rectangular A500 steel

Description	Symbol	Value
Modulus of Elasticity	E	19994.80 KN/cm^2
Shear Modulus	G	7722.13 KN/cm^2
Poisson's ratio	V	0.30
Specific weight	γ	77.00 KN/m^3
Thermal coefficient of expansion	α	1.20 x 10^{-5} 1/℃
Yield limit	F_y	26.89 KN/cm^2
Last Stand	F_u	31.03 KN/cm^2

Table 2. Mechanical properties of Galv 6x7 Wc cable

Description	Symbol	Value
Modulus of Elasticity	E	9000.00 KN/cm^2
Shear Modulus	G	3000.00 KN/cm^2
Poisson's ratio	V	0.500
Specific weight	γ	87.31 KN/m^3
Thermal coefficient of expansion	α	1.20 x 10^{-5} 1/℃
Last Stand	F_u	177.00 KN/cm^2

In cables, these work in tension with a non-linear behavior. Table 2 shows the mechanical properties of the 6x7 Wc spiral type galvanized cable, and the corresponding choice is due to the common use in industrial constructions since it is exposed to cross winding and maintains its mechanical integrity without deformation in compliance with the UNE-EN 12385-4 certification [13].

In the tensioned roof, it is the main material that supports gravity and wind loads. It produces deformations on the surface and its behavior is tensile [14]. For the investigation, a textile membrane (FR 900 - Type II) was used (see Table 3).

Table 3. Mechanical properties of stretched canvas

Description	Value
Tensile strength warp/weft	4300/4200 N/50mm
Tear strength warp/weft	500/500 N
Crack resistance	100,000 T-no craks
Total weight	700 g/m^2
Thickness	0.8 mm
Base fabric	Polyester Panama Weave P2/2
Type of coating	PVC
Finish	Nanopolymered fluorinated lacquer, Multi-composed PVDF-lacquer system on both sides, antimicrobial, UV-protected, Titanium dioxide (TiO_2) front side primer

Loads and combinations were assigned, using the load and resistance factor design (LRFD) method in conjunction with allowable stress design (ASD) method to have an optimal and reliable design [15]. The load combinations for LRFD and ASD are presented in Table 4 below.

Table 4. Table combination of LRFD and ASD loads

Type	Combinations
VERIFICATION ASD	1.4D
	1.2D+1.6(Lr o S o R)
	1.2D+1.6(Lr o S o R) +(L o 0.5W)
	1.2D+W+L+0.5(Lr o S o R)
	0.9D+W
	1.2S+Ey+Eh+L+0.2S
	0.9D+Ey+Eh+L
VERIFICATION LRFD	D
	D+L
	D+ (Lr o S o R)
	D+0.75L+0.75 (Lr o S o R)
	D+0.6W
	D+0.75L+0.75(0.6W) +0.75(Lr o S o R)
	0.6D+0.6W
	D+0.7E_v+0.7E_h
	D+0.525E_v+0.525E_h+0.75L+0.75S
	0.6D-0.7E_v+0.7E_h

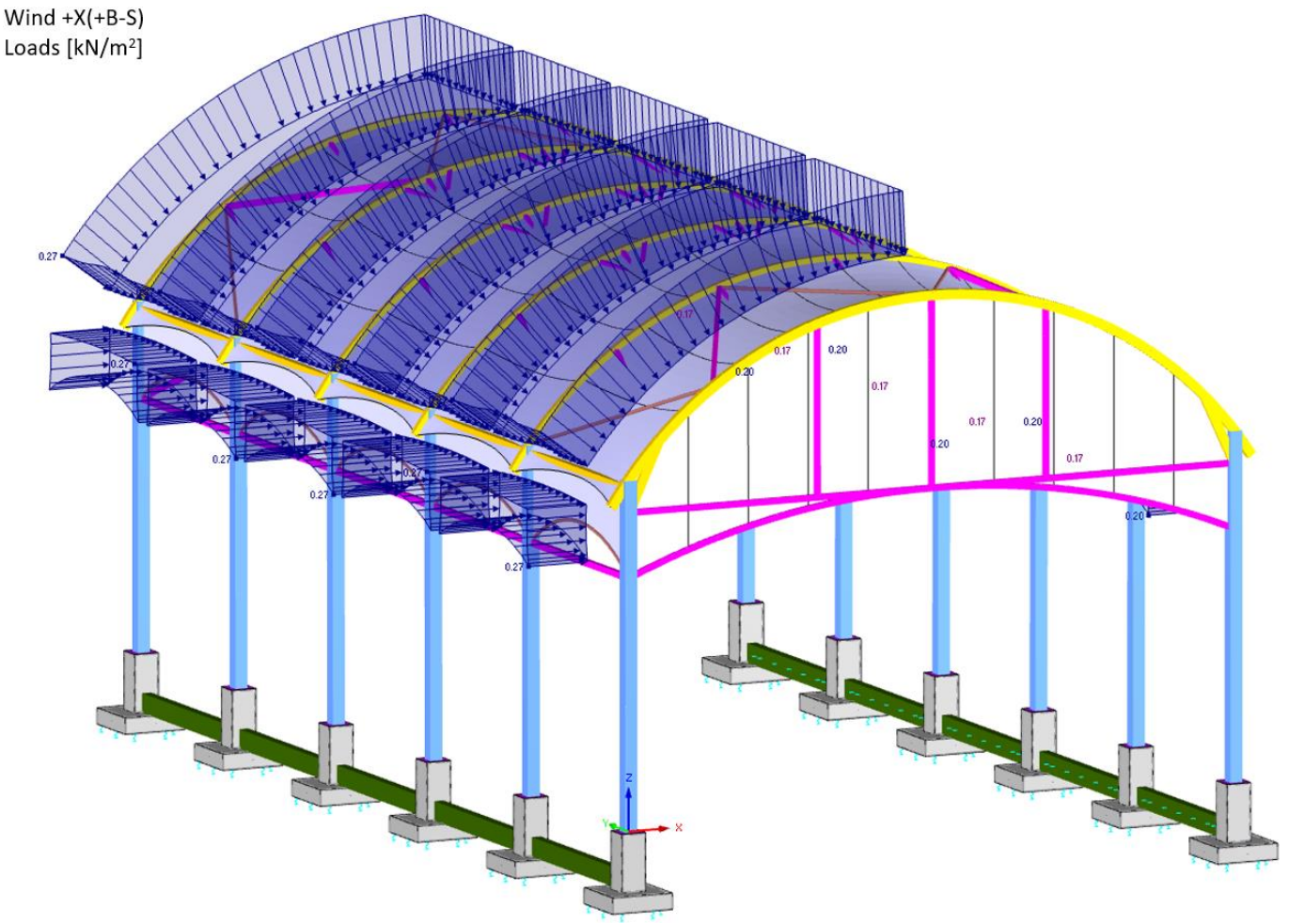

(a)

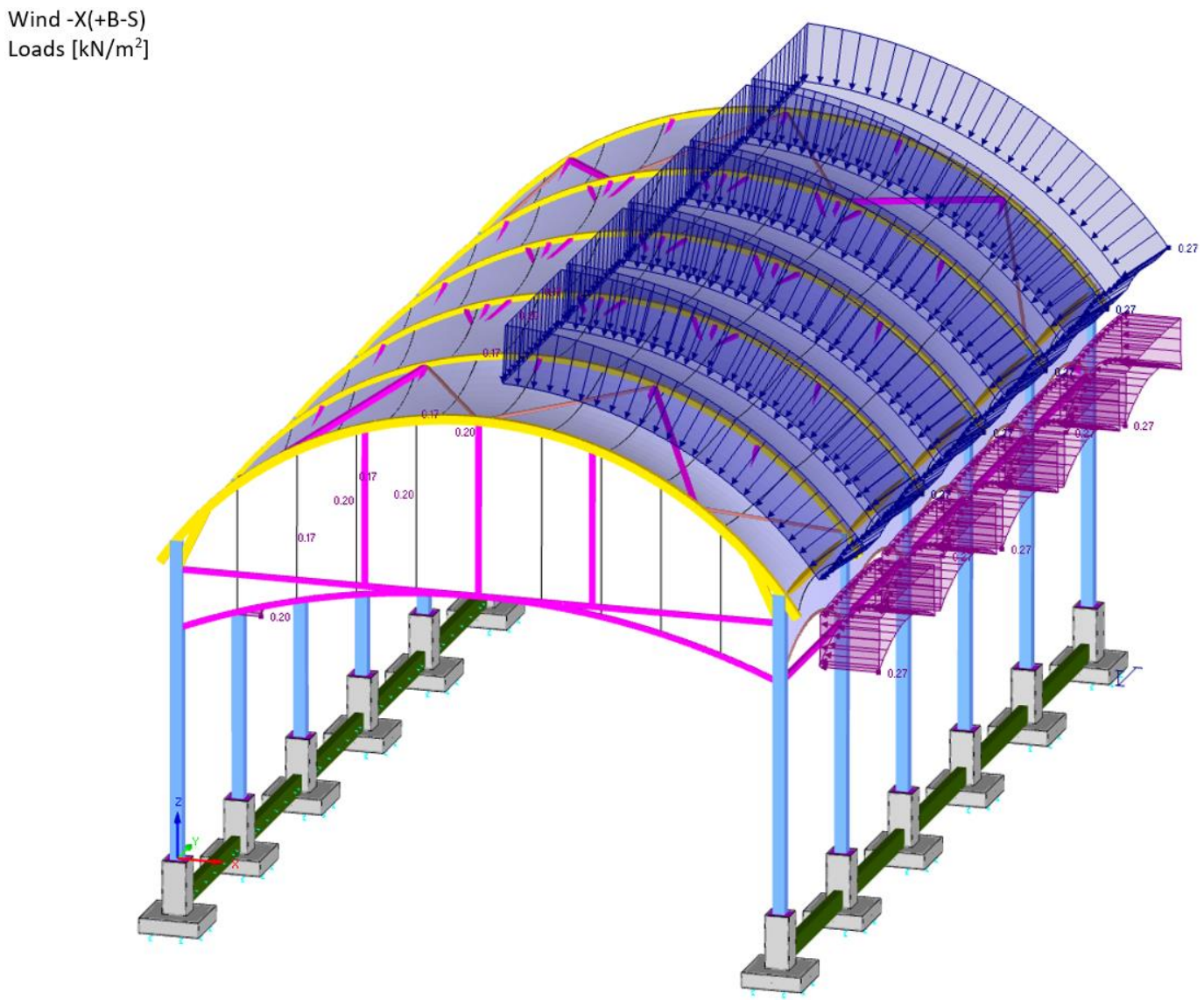

(b)

Figure 2. Allocation of loads on the structure (a: Wind load in the +X direction; b: Wind load in the -X direction)

Where: “D” is the dead load, “Lr” is the reduced live load, “S” is the snow load, “R” is the rain load, “W” is the wind load, “Ev” is the earthquake load in the horizontal direction and “Eh” is the earthquake load in the vertical direction. An example of load assignment in +X and -X direction for the structure is shown in Figure 2.

2.3. Tensile Structure

The tensile structures reach equilibrium by pure traction; for this purpose, their geometry is modified until an anticlastic surface is obtained [16]. That is, the force of gravity is counteracted by the internal air pressure and the upward forces resisted by tension [4], as shown in Figure 3.

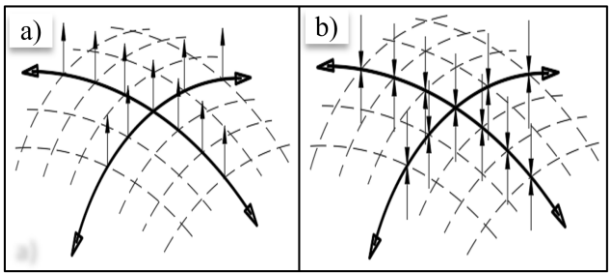

Figure 3. Loads in both directions on anticlastic surface (a: upward loads resisted by tension; b: gravity loads balanced by the internal force of air)

2.4. Geometric Nonlinear

Geometric nonlinearity is generated when the hypothesis of small displacements is not applicable; therefore, the superposition principle is not applicable [17]. Therefore, tensile structures resist gravity loads, large displacements, and rotations [4].

2.5. Form Search

It aims at maintaining the geometry for different loads and excessive deformations against wind. For this purpose, the dynamic relaxation method focuses on analyzing the nonlinearity without any added effort.

2.6. Wind Tunnel Method

The Wind Tunnel methodology in the RFEM 5 software employs a wind flow analysis that is relatively close to real situations, thus helping to parameterize the dynamic behavior at different loads and providing a numerical simulation of the structure [18]. After entering the properties of each material defined in Tables 1, 2 and 3 together with the load actions defined in Table 4 in the RFEM 5 software, we continued with the generation of the Finite Element mesh (see Figure 4) with a mesh density of 20% and level of detail 2, considering the shape search of the surface under tension by means of the linear force density method (FDM). It replaces the surface with a mesh of cables for the equilibrium shape of the surface. Having the final shape, the boundary conditions and the cables were assigned to pre-stiffen the deck, also, the realization of the virtual displacements was made compatible with the supports for kinematic boundary conditions (homogeneous or heterogeneous in order not to produce additional displacement on the supports.

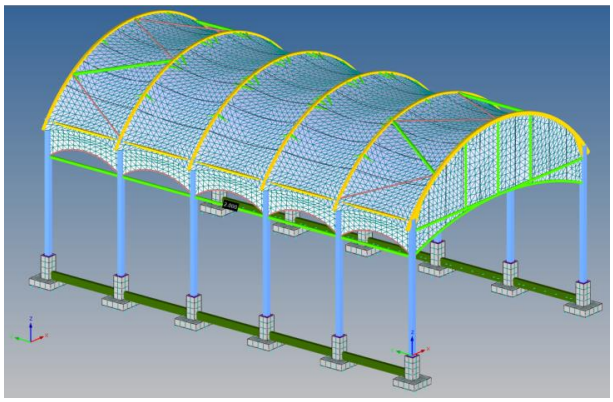

Figure 4. Assignment of finite elements

The investigation culminated with computational fluid dynamics (CFD) wind tunnel analysis of turbulent flow throughout the structure as shown in Figure 5, using the SIMPLE algorithm based on the Navier-Stokes equations to solve nonlinear models [19]. Meshing is directly related to the quality of the results, the tensile deck is discretized for each segment following a pattern, that is why the structure employs displacement vectors {u}, normal stresses {σ}, tangential stress {τ}, unit strain {ε} and rotation {γ} encompassed by the RWIND software. Likewise, in order to address the ductile behavior of the material and ensure the maximum stress does not exceed the bending stress, the Richard Von Mises principle is used.

Four portal frame models were used (see Table 5), each analyzed for wind directions at 0 °, 90 °, 180 ° and 270 °.

To simulate, the RWIND software started the process with the appropriate characterization of the wind flow, a kinematic viscosity of 0.000015 m^2/s, an air density of 1.834 kg/m^3, and a propagation velocity according to equation 8 for different heights and flow intensities [20]. After defining the wind flow, it is essential to consider the boundary conditions using the triangular mesh.

$$V(z) = \sqrt{\frac{2*q(z)}{\rho}} \tag{8}$$

Where “V(z)” is inlet velocity, “q(z)” is peak velocity pressure and “ρ” is air density.

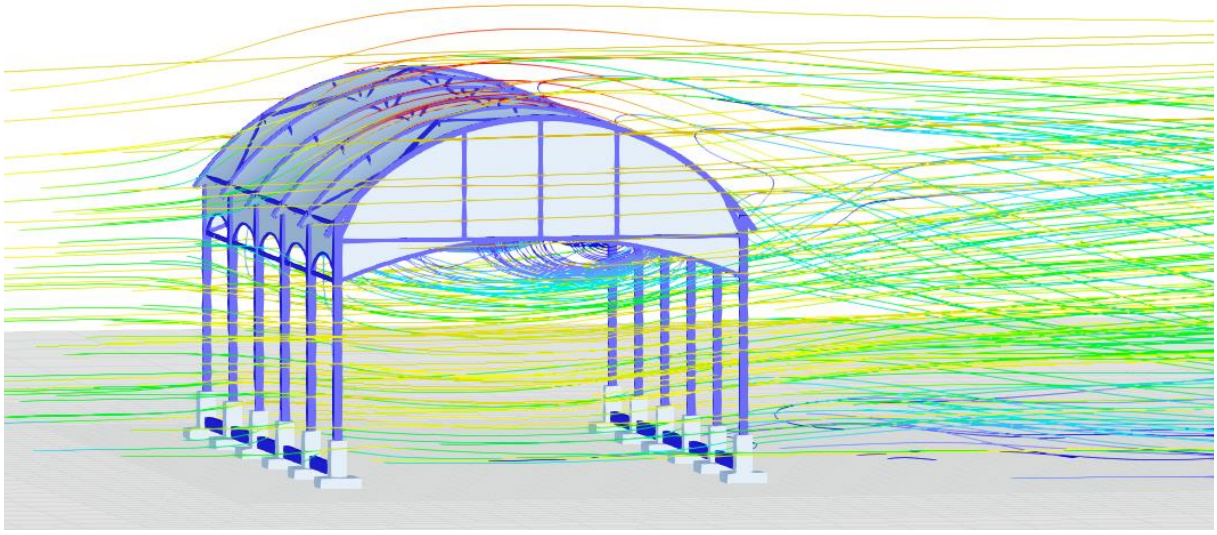

Figure 5. Wind Tunnel Experiment

Table 5. Wind tunnel analysis models

N °	TYPE	X AXIS	Y AXIS	NOMENCLATURE
01	METAL STRUCTURE	2 PORTOCASES	2 PORTOCASES	MODEL 2 PORTOCASES
02	METAL STRUCTURE	2 PORTOCASES	4 PORTOCASES	MODEL 4 PORTOCASES
03	METAL STRUCTURE	2 PORTOCASES	6 PORTOCASES	MODEL 6 PORTOCASES
04	METAL STRUCTURE	2 PORTOCASES	8 PORTOCASES	MODEL 8 PORTOCASES

3. Results

3.1. Displacement

Figure 6 shows the displacements of the 2, 4, 6 and 8 portal frames. The 6 and 8 portal frames show lower values in both the static analysis and the wind tunnel, reaching maximum values of 227.4 mm and 250.20 mm, respectively, while the value for the 2-portal frame model was higher in the wind tunnel.

3.2. Tension Forces

In Figure 7, the tensile strength of the coverings of the 2, 4, 6 and 8 portal models is observed, having a constant value of 0. 43 KN/cm^2 for wind tunnel in the 2, 4, 6 and 8 portal models, however, there were variations in the tension force for the static analysis, where the 6 and 8 portal models presented an increase in the tension force of 2.17% with respect to the 2 and 4 portal models, since the 2 portal models had the lowest tensions.

3.3. Safety Factor LRFD and ASD

Figure 8 shows the LRFD verifications of the 2, 4, 6 and 8-frame models with an average ratio of 0.75 for the static analysis and an average ratio of 0.77 for the wind tunnel. Likewise, the 6- and 8-frame static models showed a good performance to the safety factors, with average values of 0.81 and 0.87, respectively, while for the 2-frame static model, the value was 0.73, thus showing a weaker configuration. Similarly, Figure 8 shows the ASD verification of the 2, 4, 6 and 8 portal frames with an average ratio of 0.66 for static analysis and an average ratio of 0.53 for wind tunnel. Likewise, the highest ratio was obtained in the 8-frame model of 0.87 for static analysis and the lowest in the 2-frame model of 0.27 for static analysis; these values reflect that for static analysis and wind tunnel the 6-frame and 8-frame models show a more preventive factor with respect to the 2-frame models.

3.4. Wind Speed

In Figure 9, the wind speed for different directions 0 °, 90 °, 180 ° and 270 ° is observed, having a minimum variation of 0.33% in the 2-portal model for the wind direction of 90 ° and 270 ° and a minimum variation of 0.35% in the 2-portal model for the wind direction of 0 ° and 180 °. However, the maximum velocity is 35.93 m/s for the 0 ° and 180 ° wind direction in the 8-frame model, and the minimum velocity is 27.22 m/s for the 90 ° and 270 ° wind direction in the 8-frame model.

3.5. Wind Pressure

In Figure 10, the wind pressure for different directions

0 °, 90 °, 180 °and 270 °is observed. However, the maximum pressure is 1431.7 Pa for the 90 ° and 270 ° wind direction in the 2-portal model, and the minimum velocity is 765.1 Pa for the 0 °and 180 °wind direction in the 2-portal model. An increase in pressure of 330.2 Pa is also observed for the 0 ° and 180 ° wind direction in the 6-frame model with respect to the 2-frame model. Therefore, the 2-frame model faces a higher-pressure load, which makes it more sensitive, while the 6- and 8-frame models retain lower pressures.

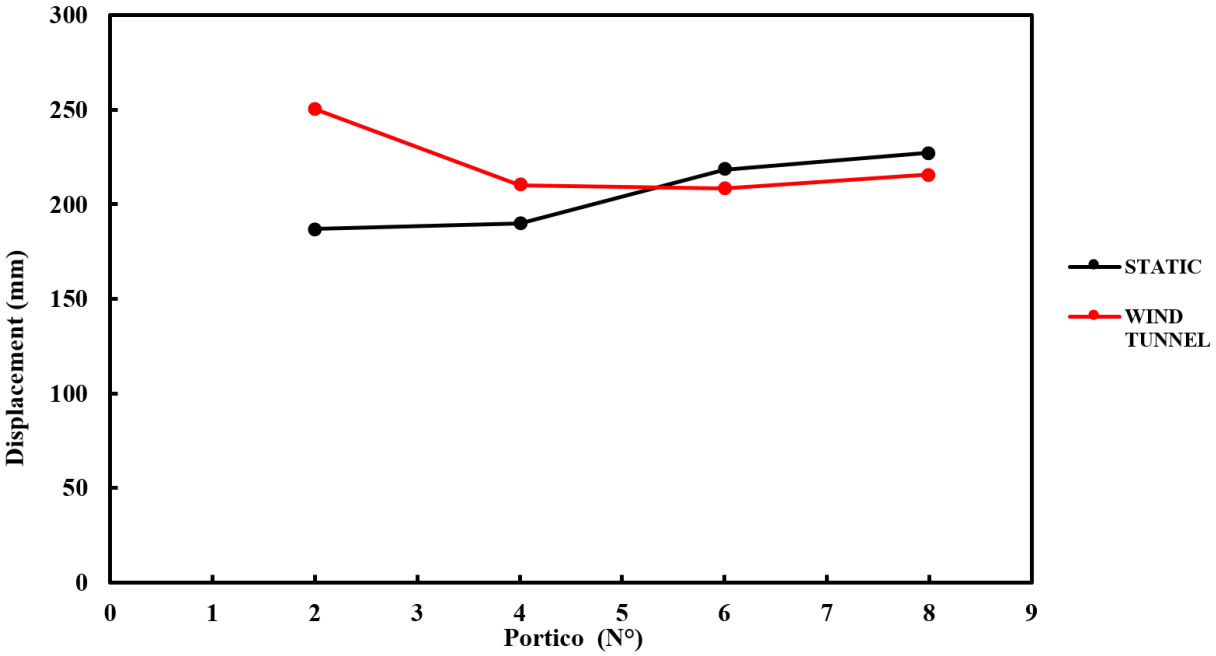

Figure 6. Travel results

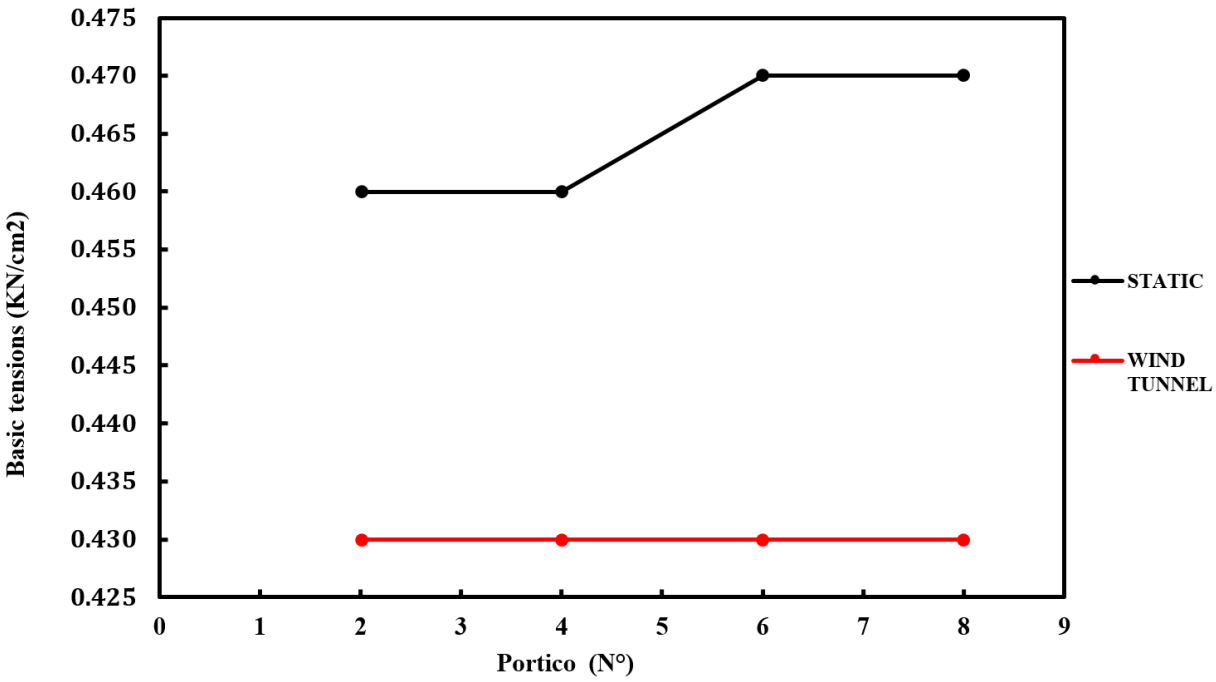

Figure 7. Tensile strength results

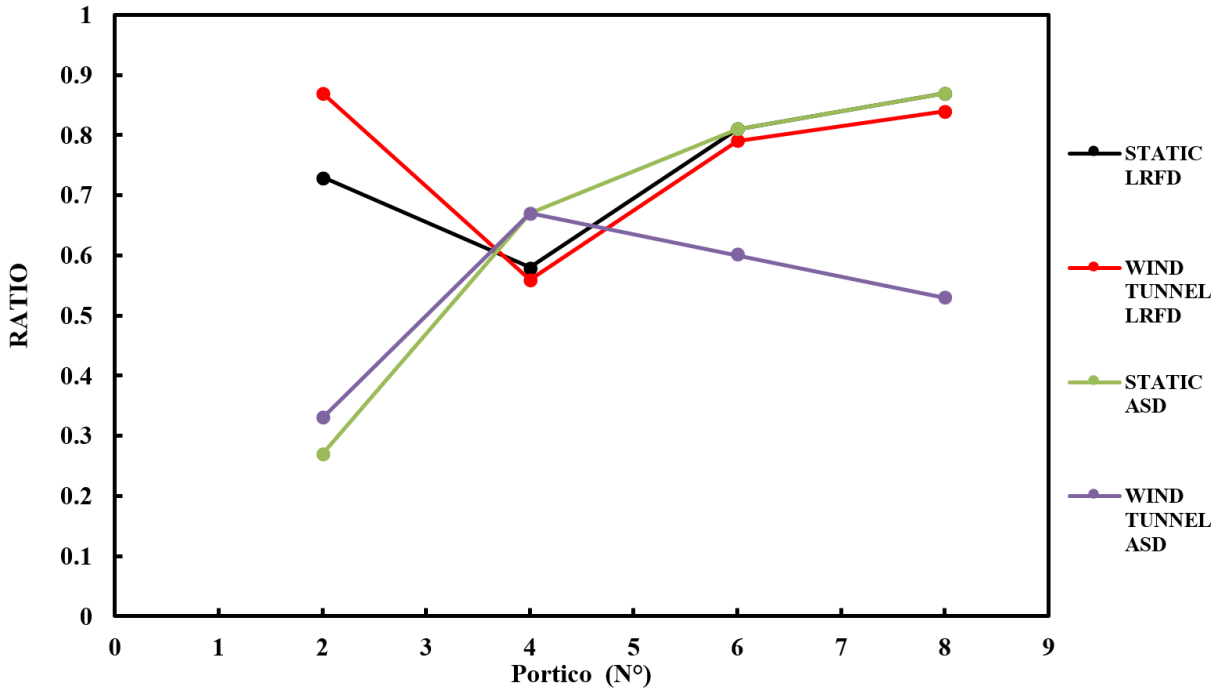

Figure 8. LRFD and ASD verification

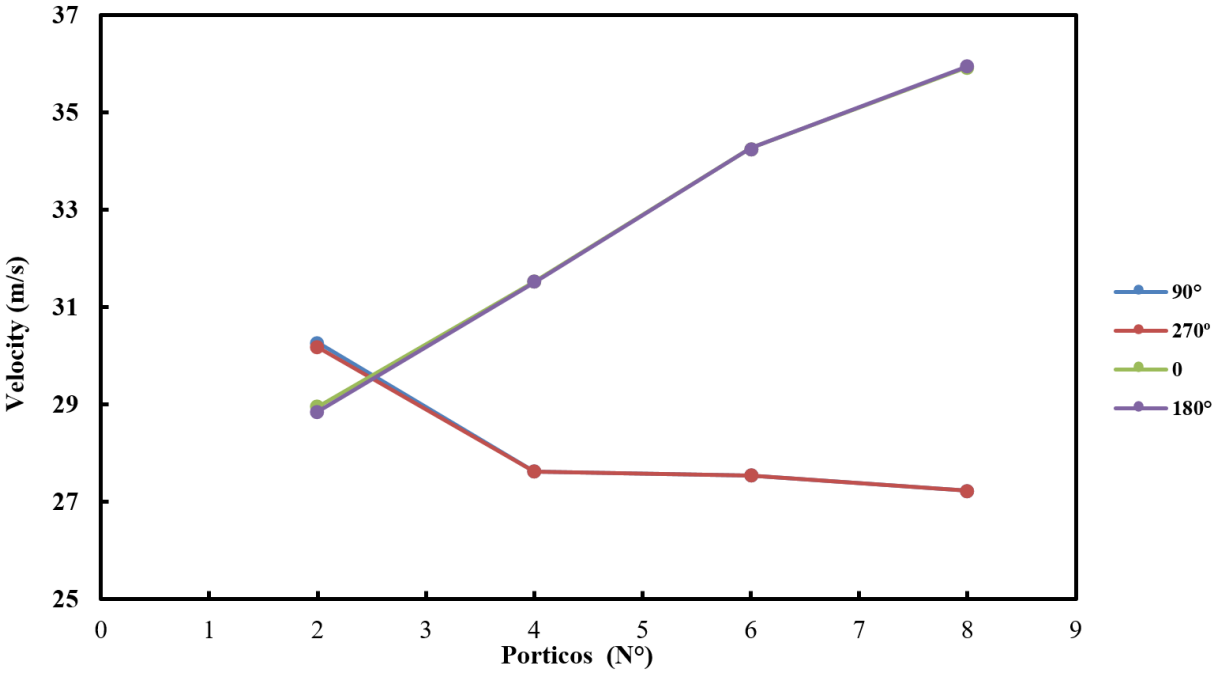

Figure 9. Wind speed

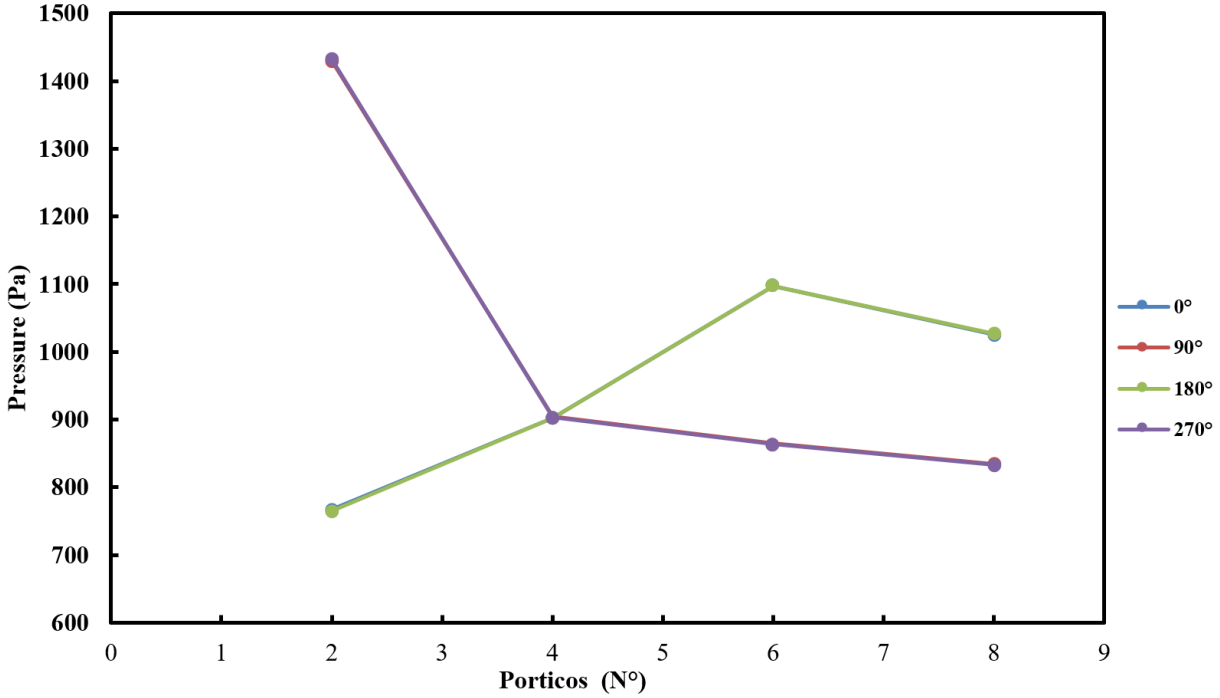

Figure 10. Wind pressure

4. Discussions

Experimental models revealed that the number of frames significantly influences displacements, tensile strength, factor of safety, wind speed and wind pressure. However, at present, there is limited information on tensile structures with parabolic steel shells against wind loads [18], which is why in this research its significance for its modeling in parabolic shells is evidenced. NTP E.020 [21] establishes the design for static wind analysis to resist windward and leeward loads in type 1, 2 and 3 buildings (classified by height, slenderness and aerodynamic difficulties). For that, I determine the design speed (see equation 1) as a function of the height not greater than 10m and a speed according to geographical area not less than 75 km/h, then use the wind pressure considering the ratio of the form factor "C" (windward: ±0.8 and leeward: -0.5) for external and internal loads "C" (windward and leeward: ±0.3) in arches and cylindrical roofs with an angle of inclination not greater than 45 º. On the other hand, in the Australian standard [22], it uses static wind analysis at heights not greater than 200 m and roof spans less than 100m determining the wind speed by establishing criteria of the factors V_R (multidirectional regional speed), M_d (wind direction for regions A1-A7) and W (0.80-1. 00), B, CyD (0.95-1.00, F_D=1.1 and F_C=1.05), M_(Z,cat) (category 1: free terrain, category 2: obstruction from 1. 5m to 10m, category 3: obstruction from 3m to 5m and category 4: obstruction from 10m to 30m and more), M_s (drindage shall be 1.0 for slope ≥12.0 and 0.7 for slope ≤1.5) and M_t (topography factor 1.0 -1.71). Next, the wind pressure was determined as a function of ρ_air (air density: 1.2kg/m^3), V_des (orthogonal design velocities of 0 º, 90 º, 180 º and 270 ºfor a height less than 25m), C_fig (aerodynamic shape factor), C_dyn (dynamic response factor). Being, AS-NZS 1170.2:2021 which employs factors such as wind direction for regions with values of 0.8-1.00, obstructions factor for different heights from 0m to plus 30m, slope(s) from 1 to ≥12.0m and topography from 1.0-1.71. But little information on pressure coefficient for arches and cylindrical shells compared to NTP E.020. Likewise, in the research [2], it does not specify a procedure to amplify the static loads to pass to the dynamic analysis. The AS-NZS 1170.2:2021 standard has better design criteria to obtain more conservative data compared to the Peruvian Technical Standard E.020. The displacements (see Figure 6), an average displacement of 227.4 mm was obtained for static analysis and 250.2 mm for wind tunnel in the taut parabolic structure at a wind speed of 23.1 km/h at 15.9 m height. Likewise in the research [5], the average displacement is 10mm in the most critical side with a speed of 40 km/h for 0 ºat 3.5 m height. Due to the square base and differences in heights where the data was taken, the average displacement is lower, making the data more truthful for wind tunnel dimensions of 4m x 4m x 4m. It was found that the tensile strength (see Figure 7), in the static analysis there is a significant increase from 0.46 KN/cm^2 to 0.47KN/cm^2 in its tensile strength value versus 0.43 KN/cm^2 for wind tunnel in the 2, 4, 6 and 8 gantry models in 1mm thickness. From the above results, an unstable and unbalanced behavior of the static analysis versus the wind tunnel is evident. Since, the finite elements, the form finding, the density force and the nonlinearity are proportional to the membrane work only in tension for the

wind tunnel; therefore, its constant value compared to the static analysis is shown in Figure 11. Likewise, in the research [2], a tensile force of 0.774 KN/cm^2 was obtained in ANSYS for a thickness of 0.9mm, and this variation is due to the fact that the tensile forces in the research were discretized with a triangular/rectangular mesh, E=1400 KN/cm^2, V=0.66 with ANSYS software versus E=50.50 KN/cm^2, V=0.458 with RFEM 5 software.

The LRFD safety factor (see Figure 8) obtained for the static analysis in the 4, 6 and 8 portal frame models is a slightly higher average ratio of 0.75 versus 0.73 for the wind tunnel, it was found that the number of portal frames for static analysis and wind tunnel guarantees the safety of the structure with a maximum ratio of 0.87. Similarly, the ASD safety factor (see Figure 8) obtained for the static analysis in the 2 and 8 portal models there is an exponential growth in the ratio from 0.27 to 0.87, furthermore the ratio of 0.67 is constant for both static and wind tunnel analysis, while in the 6 and 8 portal model there is a drop in the ratio from 0.60 to 0.53 for wind tunnel. The research [23] mentioned that the safety level in ASD is less reliable than LRFD and failure acceptances are higher than LRFD. Because for ASD and LRFD (see Figure 8) the superiority of ASD over LRFD is evidenced. On the other hand, the Peruvian standard E020 [11], does not consider more specific dependent variables such as topography factor, aerodynamic shape factor, dynamic response factor to parameterize in functions to the study area and establish an improvement in the behavior of the structure according to the design speed, as well as the European standard that only contains very poorly defined parameters [18].

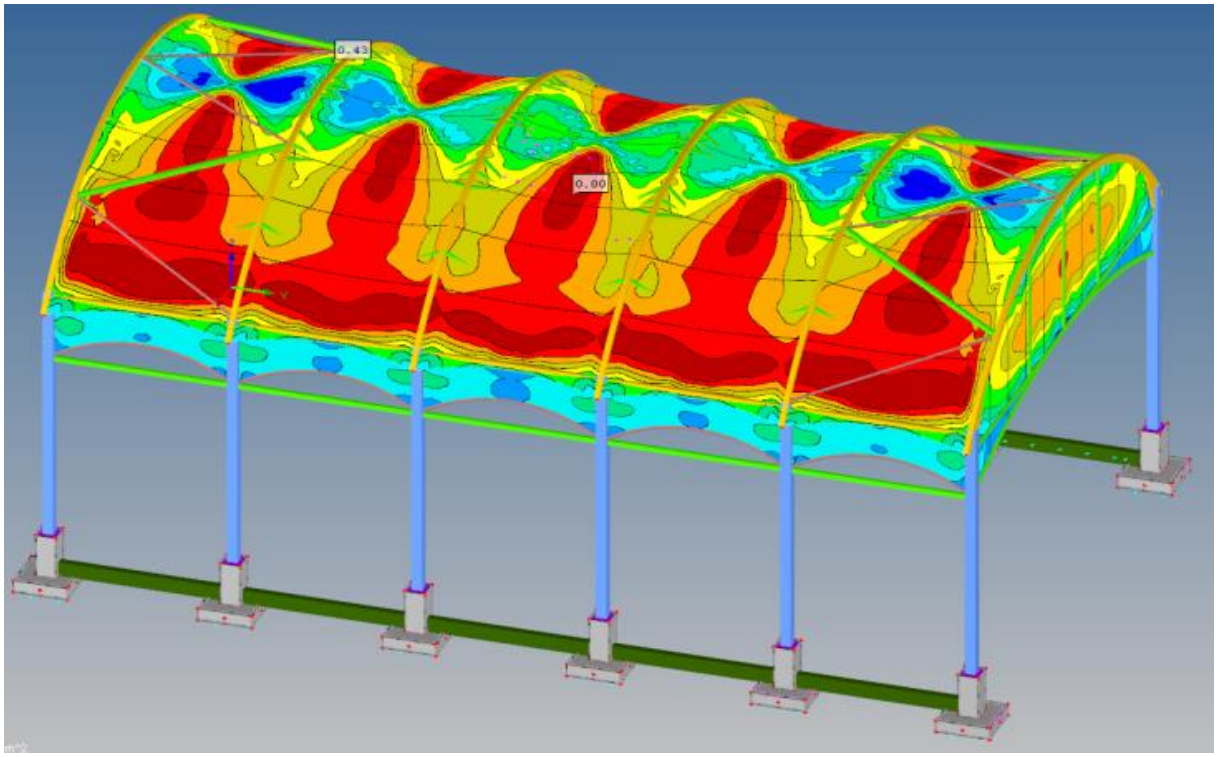

Figure 11. Wind tunnel stress forces in the 6-frame model

5. Conclusions

In tensile system structures, the number of frames significantly influences the dynamic response such as displacements, tension forces that guarantee safety, and a resistance of the materials to different loads in low temperature climates with a useful life of approximately 50 years; however, preventive maintenance must be taken into account to guarantee stability, since the deterioration of the materials is affected after 5 years due to climatic changes.

To perform the wind tunnel simulation it is important to start from the design criteria of static wind analysis in each standard to subsequently validate under a dynamic finite element approach and non-linear geometric wind tunnel, thus amplifying and projecting the values to obtain a better response of the tensile system structure against loads in different situations, performing the static analysis and wind tunnel ensures an almost real simulation of the structure in unfavorable conditions providing the professional with a better interpretation of results.

Based on the results and the pressure coefficient Cp established by the standard that was processed in RFEM 5 and RDWIN, it was obtained that the velocity is directly proportional to the number of frames for the direction (0 º and 180 º) and inversely proportional to the number of frames for the direction (90 º and 270 º). In summary, the most dangerous wind speed is in the direction (0 ºand 180 º) producing significant displacements, which at the time of designing a tensile structure system should have a greater incidence in the analysis of this direction and in the opposite directions a less exhaustive analysis since they produce slight vibrations. The distribution of pressures in the membrane was considered important for each portal frame model, it is known that in the most critical direction (0 ºand 180 º) there is a significant control of the pressure, despite the area and force exerted by the wind in that direction.

For future research, it is recommended to use measurement sensors at different angles and heights to compare displacements, stresses and strains insitu versus wind tunnel. In addition, the structure should not be analyzed in isolation, but within a radius of 100 m to consider adjacent buildings and vegetation; on the other hand, it is recommended to update the wind design criteria for Peruvian technical standard E.020 and implement wind dynamics.

REFERENCES

[1] E. Muñiz Martín and R. Sastre Sastre, “Dynamic analysis of tensile structures: proposal of a calculation methodology and applied software”, Universitat Politècnica de Catalunya, 2014. doi: 10.5821/dissertation-2117-95573.

[2] L. E. Pech Lugo, “Parametric study of the effects of wind on a tensile structure”, 2016, Accedido: 14 de octubre de 2024. [En línea]. Disponible en: http://www.ptolomeo.unam.mx:8080/xmlui/handle/132.248.52.100/10133

[3] L. Herrera and B. Filiberto, “Design methodology for tensile structures applied in greenhouses”, Thesis, Universidad Autónoma de Aguascalientes, 2018. Accedido: 14 de octubre de 2024. [En línea]. Disponible en: http://bdigital.dgse.uaa.mx:8080/xmlui/handle/11317/1596

[4] M. Asghari Mooneghi and R. Kargarmoakhar, “Aerodynamic Mitigation and Shape Optimization of Buildings: Review”, *Journal of Building Engineering*, vol. 6, pp. 225-235, jun. 2016, doi: 10.1016/j.jobe.2016.01.009.

[5] D. Marchisotti, P. Schito, and E. Zappa, “3D Measurement of Large Deformations on a Tensile Structure during Wind Tunnel Tests Using Microsoft Kinect V2”, *Sensors*, vol. 22, no. 16, Art. no. 16, ene. 2022, doi: 10.3390/s22166149.

[6] S. J. P. Blanco and K. Hincz, “Computational Wind Engineering of a Mast-supported Tensile Structure”, *Periodica Polytechnica Civil Engineering*, vol. 66, no. 1, Art. no. 1, 2022, doi: 10.3311/PPci.18656.

[7] F. Rizzo, F. Speziale, and S. GEYER, “Aerodynamics of Tensile Structures”, *Proceedings of IASS Annual Symposia*, vol. 2014, no. 6, pp. 1-8, sep. 2014.

[8] O. Hubová, M. Macák, M. Franek, O. Ivánková, and L. B. Konečná, “Implementation of Data from Wind Tunnel Tests in the Design of a Tall Building with an Elliptic Ground Plan”, *Buildings*, vol. 13, no. 11, Art. no. 11, nov. 2023, doi: 10.3390/buildings13112732.

[9] G. D. Stefanou, “Dynamic response of tension cable structures due to wind loads”, *Computers & Structures*, vol. 43, no. 2, pp. 365-372, abr. 1992, doi: 10.1016/0045-7949(92)90154-R.

[10] M. B. Vikram, G. Chandradhara, and B. Keerthi Gowda, “A study on effect of wind on thestatic and dynamic analysis”, *International Journal of Emerging Trends in Engineering and Development*, vol. 3, no. 6, pp. 885-890, 2014.

[11] SENCICO, *Loads E.020-National Building Regulations (RNE). 2020. Accessed: October 14, 2024. [Online]. Available at: https://www.gob.pe/institucion/sencico/informes-publicaciones/887225-normas-del-reglamento-nacional-de-edificaciones-rne*

[12] S. Loges, “Seismic vulnerability of tubular steel frame buildings in Venezuela”, presented in IDEC Research, Venezuela, 2016, p. 13.

[13] UNE, *-EN 12385-4:2003+A1:2008 Braided cables for general lifting applications*, 2008. Accedido: 17 de noviembre de 2024. [En línea]. Disponible en: https://www.une.org/encuentra-tu-norma/busca-tu-norma/norma?c=N0041175

[14] A. Jimenez, “Technical and economic analysis of the tenso structure as a proposal for the roof of the Atahualpa Olympic Stadium box”, phdthesis, Pontificia Universidad Católica del Ecuador, Ecuador, 2016.

[15] J. M. Han, K.-Y. Gu, K.-S. Kim, K.-W. Ham, and S.-R. Kim, “Calibration of the Resistance Factors for the LRFD of Shallow Foundations of Transmission Towers under Uplift Loading”, *International Journal of Geomechanics*, vol. 24, no. 8, 2024, doi: 10.1061/IJGNAI.GMENG-9481.

[16] M. T. Hamon C. and M. Pérez S., "Basic criteria in the analysis and design of tensile structures", Thesis, 2015. Accessed 20 October 2024. [Online]. Available at: http://saber.ucv.ve/handle/10872/11748

[17] G. Ottazzi, *COURSE NOTES STRUCTURAL ANALYSIS I*. Perú: PUCP, 2014.

[18] M. Kawulok, N. Freiherrová, M. Horňáková, D. Juračka, and M. Krejsa, "Hyperbolic Paraboloid Tensile Structure—Numerical CFD Simulation of Wind Flow in RWIND Software", *Buildings*, vol. 13, no. 3, 2023, doi: 10.3390/buildings13030681.

[19] G. Alfonsi, "Reynolds-averaged Navier-Stokes equations for turbulence modeling", *Applied Mechanics Reviews*, vol. 62, no. 4, pp. 1-20, 2009, doi: 10.1115/1.3124648.

[20] C. Kloss, C. Goniva, A. Hager, S. Amberger, and S. Pirker, "Models, algorithms and validation for opensource DEM and CFD-DEM", *Progress in Computational Fluid Dynamics*, vol. 12, no. 2-3, pp. 140-152, 2012, doi: 10.1504/PCFD.2012.047457.

[21] Ministry of Housing, Construction and Sanitation, NORMA E.020 CARGAS, 2020.

[22] J. D. Holmes, R. G. J. Flay, J. D. Ginger, M. Mason, A. Rofail, and G. S. Wood, "The 2021 Australian/New Zealand Standard, AS/NZS 1170.2:2021", *Wind and Structures*, vol. 37, no. 2, pp. 95-104, 2023, doi: 10.12989/was.2023.37.2.095.

[23] D. Akchurin, R. Sabelli, R. Ziemian, and B. Schafer, "ASD and LRFD: Reliability Comparison for Designs Subjected to Wind Loads", *Journal of Constructional Steel Research*, vol. 213, p. 108327, dic. 2023, doi: 10.1016/j.jcsr.2023.108327.